Astronomy & Astrophysics manuscript no. ms˙1
February 1, 2008

Automated search for galactic star clusters in large multiband surveys: I. Discovery of 15 new open clusters in the Galactic anticenter region

E.V. Glushkova[1], S.E. Koposov[2,3,1] and I.Yu. Zolotukhin[1]

[1] Sternberg Astronomical Institute, Universitetskiy pr. 13, 119992 Moscow, Russia
[2] Max Planck Institute for Astronomy, Königstuhl 17, D-69117, Heidelberg, Germany
[3] Institute of Astronomy, University of Cambridge, Madingley Road, Cambridge CB3 0HA, UK
S. Koposov e-mail: koposov@mpia.de, E. Glushkova e-mail: elena@sai.msu.ru

Received ¡date¿ /Accepted ¡date¿

ABSTRACT

Aims. According to some estimations, there are as many as 100000 open clusters in the Galaxy, but less than 2000 of them have been discovered, measured and cataloged. We plan to undertake data mining into multiwavelength surveys to find new star clusters.
Methods. We have developed a new method to search automatically for star clusters in very large stellar catalogs, which is based on the convolution of the density maps with different kernels. We have applied this method to a subset of the 2MASS catalog towards the Galactic Anticenter.
We also developed a method to verify whether detected stellar groups are real star clusters, which tests whether the stars that form the spatial density peak also fall onto a single isochrone in the color-magnitude diagram. By fitting an isochrone to the data, we estimate at the same time the main physical parameters of a cluster: age, distance, color excess.
Results. For the present paper, we carried out a detailed analysis of 88 overdensity peaks detected in a field of 16×16 degrees near the Galactic Anticenter. Physical and structural parameters were determined for 12 of 15 newly discovered clusters and for 14 yet-unstudied known open clusters thus almost tripling the sample of open clusters with studied parameters in the anticenter. The parameters determined with this method showed a good agreement with published data for a set of well-known clusters.

Key words. Galaxy: structure - open clusters and associations:general - Surveys - Catalogs

1. Introduction

Star clusters are unique laboratories for investigation of a wide range of astrophysical problems relating to star formation, stellar evolution, the formation and structure of the Milky Way, and the distance scale of the Universe. As star clusters are usually single-age and single-metallicity populations, distance, age, and reddening in the cluster's direction can be determined with much higher accuracy then for isolated, or "field", stars. To define at least a reliable ranking of the open cluster properties, we need a large sample of objects whose age, distance, and metallicity are accurately and homogeneously known. So far, 1756 open clusters have been cataloged (Dias et al., 2002), but the basic physical parameters are known for less than 700 objects. And all these parameters have been derived by different authors based on heterogeneous observational data. Most of the open clusters in the Galaxy have probably not yet been found, because open clusters are concentrated near the Galactic plane where extinction by interstellar dust is most severe. Some literature estimates put the total number of open clusters in the Galaxy at 10^5 (see, for example Surdin (2000)). Modern all-sky surveys (e.g. 2MASS, DENIS, SDSS, etc.) provide a large store of information to study open clusters comprehensively and homogeneously. Near-infrared surveys are especially useful, because the data are far less affected by high reddening in the Galactic plane where the most open clusters are located.

Numerous attempts have been made in recent years to search for star clusters using such large surveys. However, total number of newly discovered clusters with robust determinations of their physical parameters does not exceed two dozen. Dutra et al. (2003) performed a visual search for IR clusters and similar objects in the direction of known nebulae, using the 2MASS Atlas and found 179 embedded clusters and stellar groups. However, it proved impossible to find the physical parameters of this type of objects through isochrone fitting. Ivanov et al. (2002) and Borissova et al. (2003) found 11 peaks by automated algorithm and 3 peaks by visual inspection in the apparent stellar surface density in 2MASS point source catalog. They detected mostly embedded IR clusters, so the physical parameters could be derived only for one object. Drake (2005) performed an automated search for clusters in USNO-A2 using the method developed by Ivanov et al. (2002) and found 8 new candidates. However, their basic parameters were not derived. Kronberger et al. (2006) visually inspected DSS and 2MASS images and selected 66 candidate clusters. For 9 of 24 most probable clusters within this sample, authors determined fundamental parameters by simple fitting. Froebrich et al. (2006) used star density maps obtained from 2MASS and found 1021 new cluster candidates. The authors statistically evaluated the contamination of their sample to be of about 50% and left verification of the nature of each individual cluster for future investigations.

We have developed a new efficient method of searching stellar catalogs for star clusters of different radii, based

Send offprint requests to: E. Glushkova, e-mail: elena@sai.msu.ru

on the convolution of the cataloged stellar source density maps with Gaussians (similar method was used to search for dwarf Spheroidal galaxies and globular clusters in SDSS; Koposov et al. (2007a,b)). The method automatically finds cluster candidates and then confirms them by testing whether the spatially clustered, potential cluster members lie on the same isochrone in the color-magnitude diagram. At the same time, this procedure determines the basic cluster parameters (age, radius, distance and color excess) by fitting the isochrone position. Below, we describe our method of automatic search for stellar overdensities and the results of its application to the 2MASS data in the field of 16×16 degrees in the region of the Galactic anticenter.

2. Method of automated search for stellar overdensities

This work aims to provide a fast, simple and efficient method of identifying open clusters in very large photometric catalogs, such as 2MASS, SDSS, DENIS etc. The overall density of the stars in the Milky Way is high at low latitudes and can vary rapidly because of dust etc. So, it is not easy to find star clusters algorithmically on such a complex background. Even when a peak is found, it is important to check whether the candidate is indeed an evolutionally connected group of cluster members or merely a group of stars clustered by chance.

Therefore, the method must be capable to detect density peaks on a sharply changing background and to evaluate their statistical significance. To develop a universal technique for all data sources, we have to make it independent of any pixelization effects and thus applicable to star structures of any size. To ensure this, we built a density map, which presents the number of counts in (RA, Dec) coordinates. Then, we convolved this image with a special filter demonstrated in Figure 1. The filter curve is the difference between two 2-D Gaussian profiles and has zero integral. Employing this special shape of the filter, we ensure that a flat, or even slowly changing background produces a zero signal, whereas the concentrations of stars exhibit a high signal. The family of such filters called Difference of Gaussians are well studied and used in Computer Vision science for feature detection at various scales (Babaud et al. (1986), Lindenberg (1998)). The convolution with such filter is equivalent to the subtraction of the density maps convolved with the gaussians of different widths. The density map convolved with the small Gaussian is used to detect the small scale overdensities, while the density map convolved with wider Gaussian is the estimation of local background.

The following formulae demonstrate our convolution procedure. First, we obtain the distribution of stars on the sky M(ra, dec):

$$M(ra, dec) = \sum_i \delta(ra, dec)$$

Then, this map is convolved with the filter:

$$M(ra, dec) = M(ra.dec) * (G(ra, dec, \sigma_1) - G(ra, dec, \sigma_2))$$

where $G(ra.dec.\sigma)$ is the circular 2D Gaussian with unity integral and width of σ. On the last step, we normalize the convolved map to get the statistical significances of all density fluctuations:

$$S(ra, dec) = \sqrt{4\pi}\sigma_1 \frac{M(ra.dec) * (G(ra, dec, \sigma_1) - G(ra, dec, \sigma_2))}{\sqrt{M(ra, dec) * G(ra, dec, \sigma_2))}}$$

That map S(ra,dec) shows the deviation of $M(ra.dec) * G(ra, dec, \sigma_1)$ above the background estimate given by $M(ra.dec) * G(ra, dec, \sigma_2)$. Under the assumption of Poisson distribution of sources and $\sigma_2 \gg \sigma_1$, the S(ra,dec) should be normally distributed with variance of 1. The detection of overdensities on such map is very easy and may be done by simple thresholding, i.e. to select all the overdensities more statistically significant than 5σ, we need find all the pixels on the map having $S(ra, dec) > 5$. In this work we typically used the detection threshold of 4.5 sigmas.

Note that for clusters of the size close to that of the inner Gaussian, the filter is very close to optimal. Also it is important

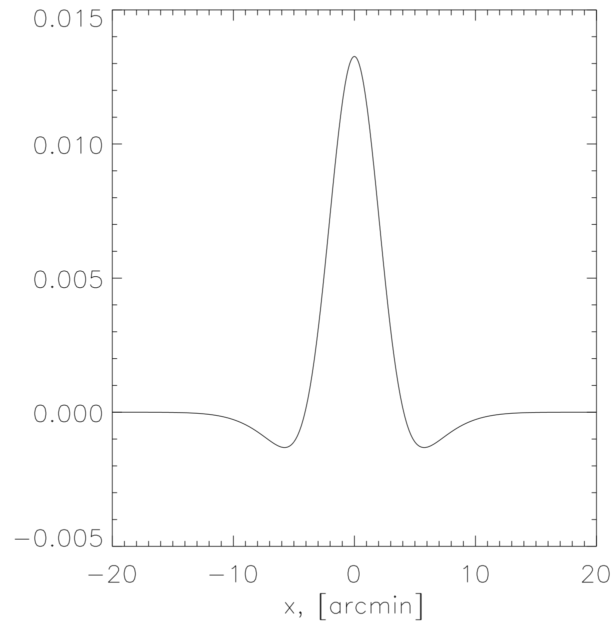

Fig. 1. The one-dimensional slice of the 2D filter which we used for the convolution for $\sigma_1 = 3'$ and $\sigma_2 = 6'$

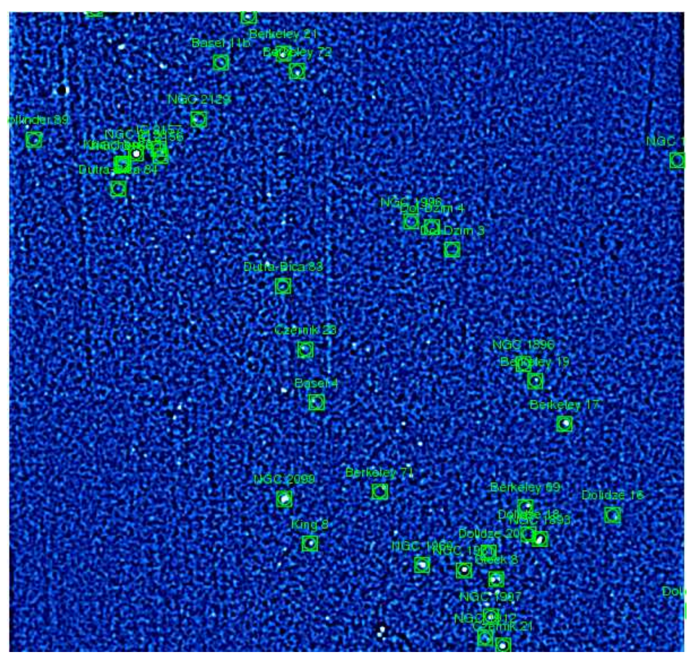

Fig. 2. The $16° \times 16°$ map of the overdensities in the anticenter region from 2MASS PSC. The known open clusters from the Dias catalog (Dias et al., 2002) are marked.

to understand that the choice of σ_2 is related to the scale on which the background estimate is obtained. Ideally, σ_2 should be rather large and much larger than the σ_1, but unfortunately the 2MASS data in the MW plane suffers significantly from the extinction and the density of stars is varying on very small scales. Therefore we are forced to use the σ_2 which is not much larger than σ_1 to have a more local estimate of the background. See also Koposov et al. (2007b) for the discussion of the method.

The example of the convolved image from 2MASS point source catalog for the $16^\circ \times 16^\circ$ anticenter region of our Galaxy is shown in Figure 2. A large population of peaks is clearly seen. As we show below, most of these peaks can be attributed to open clusters (among them, 1/3 are new).

After the density peaks are detected, each individual peak should be questioned whether it relates to a real cluster or just a random fluctuation. We can answer this question most reliably if we determine whether the density peak is associated with the stars lying on the same isochrone. For this purpose, we developed a semi-automated method of isochrone fitting. All isochrones of solar metallicity were taken from Girardi et al. (2002). To fit an isochrone, we chose, by visual inspection, the initial age and shifts along coordinate axes corresponding to the color excess and distance modulus. Then, we shifted the isochrone along coordinate axes with variable steps and changed its age with $\Delta log(age) = 0.05$. At each step, we built automatically the radial density distribution for stars lying in the vicinity of the isochrone (distance from it in the color index is less then 0.05 - assumed cluster members) and for all other stars (distance is greater than 0.05 - supposed field stars). Ideally, the distribution function for field stars should be flat, whereas the cluster members should feature a noticeable concentration towards the center. In practice, the radial density distribution of field stars shows a weak central concentration, because some peculiar cluster members may lie far from the isochrone, or the theoretical isochrone may not well fit the CMD for observational data, or because of larger photometric errors for faint stars. That is why we compared the contrast of central peaks for two distributions allowing for the errors in density and found the maximum contrast ratio. Testing our technique for well-studied open clusters, we found that the contrast ratio should be greater then 2, so we use this value to decide if the found overdensity is a real cluster or not.

3. Application of the method to the 2MASS data

The Two Micron All Sky Survey (2MASS, Skrutskie et al. (2006)) gives us a comprehensive dataset both to search for new open clusters and to test our method: it covers 99.998% of the sky with uniform precise photometry and astrometry in the J (1.25 μ), H (1.65 μ), and K_s (2.16 μ) photometric bands. The global 2MASS sensitivity is 15.8 for J-band, 15.1 for H-band, and 14.3 for K_s at $S/N = 10$. For this reason, we investigated the $(J, J-H)$ color-magnitude diagrams in our work, but also used $(K, J-K)$ diagrams to confirm found cluster parameters and be sure that the relation $E(J-H)/E(J-K)$ agrees with the normal extinction law.

To extract J, H, K_s photometry and astrometry data, we used the Virtual Observatory resource named SAI CAS (http://vo.astronet.ru), allowing us to access the largest astronomical catalogs (Koposov & Bartunov (2006)). For our purposes, we only selected the stars, which have the quality flags better than U in each filter J, H, K.

Our primary goal was to detect clusters which have diameters from few to ten arcminutes, so we used $\sigma_1 = 3'$ and $\sigma_2 = 6'$ in the filter function. The clusters having diameters more than 15-20 arcminutes do not show as a rule the visual overdensity on the sky except the most reach ones. Such extensive clusters are usually found by common proper motions or radial velocities.

As a first application, we studied a field of 16 by 16 degrees towards the Galactic anticenter and detected there 88 density peaks of $> 4.5 \times \sigma$ significance. We compared these cluster candidates with open clusters listed by Dias et al. (2002); 23 of our significant peaks can be matched to known optically visible clusters. Furthermore, 9 density peaks were matched to embedded infrared clusters from the list by Bica et al. (2003a) and Bica et al. (2003b). Dias' catalog contains additional 15 open clusters in this region, but our method does not detect them. Six of 15 clusters are not reliable clusters: they are not found in the DSS and 2MASS images, three of them are doubtful clusters according to Dias et al. (2002), one such object has no entry in database on open clusters WEBDA developed by E. Paunzen and J.-C. Mermilliod (http://www.univie.ac.at/webda/). Other 5 clusters having diameters ranged from 20 to 60 arcmin according to Dias et al. (2002), are considered as clusters by the common pattern of the proper motion of star members, and only 2 clusters among them, NGC 1912 and NGC 2168, exhibit stellar overdensities. Rest four clusters are density peaks under $4.5 \times \sigma$ significance, and three of them are seen on 2MASS images as weak embedded clusters and have no available data, except diameters, in Dias' catalog. Because more than a half of known clusters, which are on our list of detected density peaks, have unreliable or no parameter measurements, we fulfilled the detailed analysis of all 88 peaks including known clusters.

We built the Hess-diagram in $(J, J-H)$ coordinates. We plotted CMD within radius r with the value between 2 and 7 arcmin (depending of the cluster size) around the overdensity center, then we subtracted the CMD for field stars built in the ring between the two radii: $3 \times r$ and $4 \times r$. Each CMD was previously normalized to the number of stars and smoothed using a 3-pixel Gaussian. Figure 3 displays the Hess-diagram for the new open cluster Koposov 52 built within the radius of 4 arcmin around the cluster center (left-hand part) and CMD for field stars in the ring around the cluster (right-hand part). The cluster can clearly be seen on the Hess-diagram by its main sequence and red clump stars.

If a cluster-suspect manifested itself at the Hess-diagram, then we fitted its CMD with an isochrone by Girardi et al. (2002) of solar metallicity and simultaneously verified whether the detected stellar group is a real star cluster by plotting radial density distribution for stars lying on the isochrone and for all other stars. By fitting the position of the isochrone to obtain the maximum contrast on the density plot, we simultaneously found main physical parameters of a cluster: age, distance, and color excess. The fitted isochrone with the age of $log(t) = 8.95$ for Koposov 52 is shown in Figure 4. Star members are taken within the radius of 2 arcmin around its center; the position of the isochrone leads to the following estimations: $E(J-H) = 0.34$ and $(m-M)_J = 13.20$. The radial density distribution corresponding to this fitted isochrone is displayed in Fig. 5: solid circles denote the stars deviating from the isochrone by less than 0.05 magnitude in color $(J-H)$; open circles denote all other stars. The errors plotted on the datapoints are simple Poisson errors. If we define the contrast as the value of density in the center divided by that on the plateau, then the ratio of contrasts for the "isochrone" and "field" stars will be around 7.

We performed isochrone fitting on $(J, J-H)$ diagram, because there is a higher magnitude limit for J-band in 2MASS,

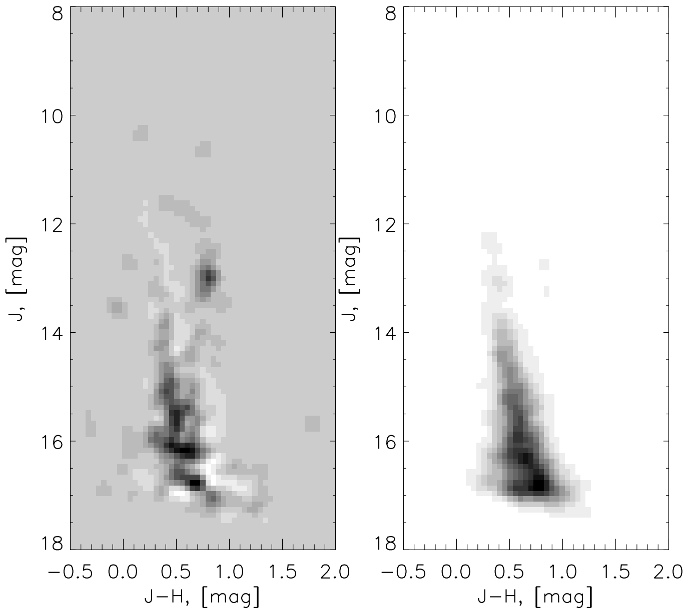

Fig. 3. Hess-diagrams for open cluster Koposov 52. The left panel shows the Hess diagram of the central 4′of the cluster with subtracted Hess diagram of the background.The right panel shows the Hess diagram of the background stars.

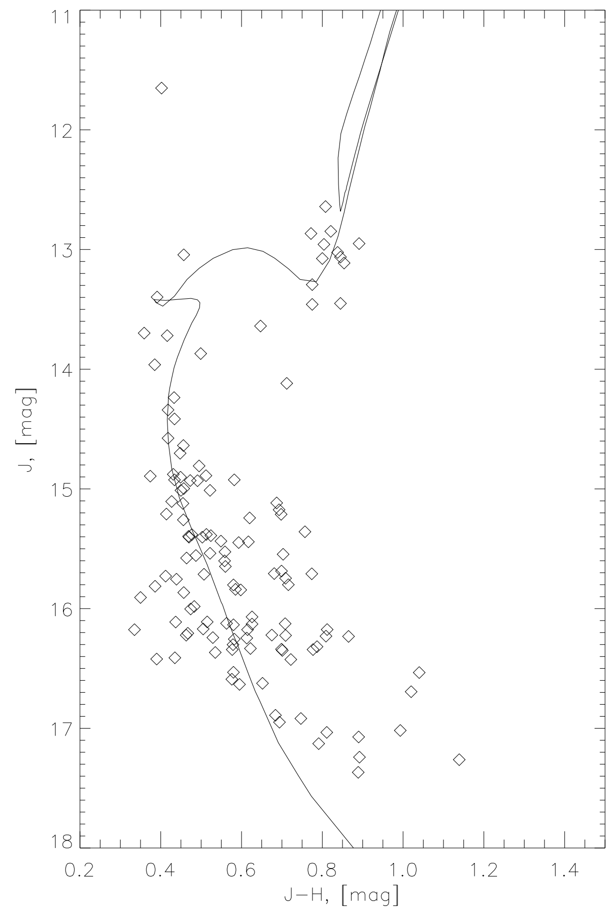

Fig. 4. Color-magnitude diagram for cluster Koposov 52 inside the radius of 2 arcminutes. The fitted isochrone with $log(t) = 8.95$, $E(B-V) = 0.04$, $(m-M)_0 = 12.32$ is overplotted.

and used a 15-arcmin region around stellar overdensity. We independently performed the same fitting procedure on a $(K, J-K)$ CMD and compared the distances obtained from two fittings with each other and the relation $E(J-H)/E(J-K)$ with the normal extinction law given by Cardelli et al. (1989), which equals to 0.55. Also we used the relations $A_{K_s} = 0.670 \times E(J-K_s)$, $A_J = 0.276 \times A_V$, and $E(J-H) = 0.33 \times E(B-V)$ from the paper by Dutra et al. (2002).

The cluster is considered to be a real cluster, if all plots (Hess-diagram, CMD, and the radial density distribution) verify the reality of the cluster.

4. Results

We used the routine described above to study all 88 overdensities. 11 stellar overdensities turn to be new optically visible clusters. One of them, Koposov 52, has been published earlier as KSE18 (Koposov et al. (2005), Zolotukhin et al. (2006)) and then independently found by Kronberger et al. (2006) as Teutsch 51. The parameters for all these clusters are listed in Table 1. The errors in color excess, distance moduli, distances and ages are evaluated from the differences in the parameters derived from isochrones fitted in $(J, J-H)$ and $(K, J-K)$ diagrams. Hess-diagrams, radial density distribution, and fitted isochrone in $(J, J-H)$ CMD's for 10 new clusters are given in Fig.6-15 in the Appendix. Five of 11 new clusters are relatively young featuring the age less than 30 Myr, whereas the other clusters in this set are very old with the age exceeding 1 Gyr. Distances of all clusters from the Sun are ranged between 1.5 and 3.5 kpc.

Also, we found 4 new infrared clusters embedded in the nebulae similar to the clusters from the list by Bica et al. (2003a) and Bica et al. (2003b): their coordinates are presented in Table 2, and Hess-diagrams are shown in Fig.16-19 in the appendix. For IR clusters, the cluster reveals itself as a cloud on the left-hand diagram; the effect of the differential extinction is also clearly noticeable. The right-hand diagram displays CMD of field stars around the cluster. Because of a high value of reddening, it was impossible to fit isochrones and find parameters for these clus-

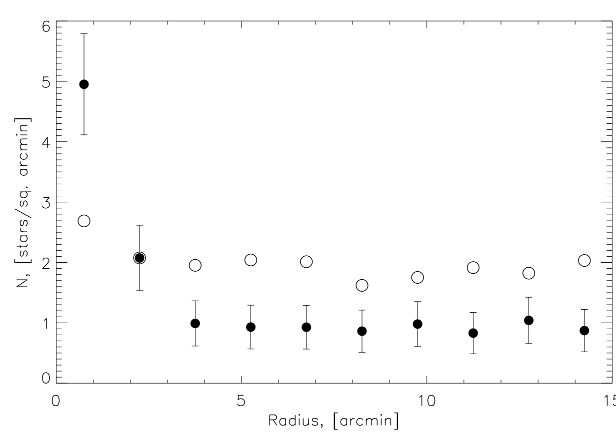

Fig. 5. Radial density distribution for stars in the field of Koposov 52. Solid circles represent the density of the stars lying closely to the isochrone. Open circles denote the density of the field stars lying far from the isochrone.

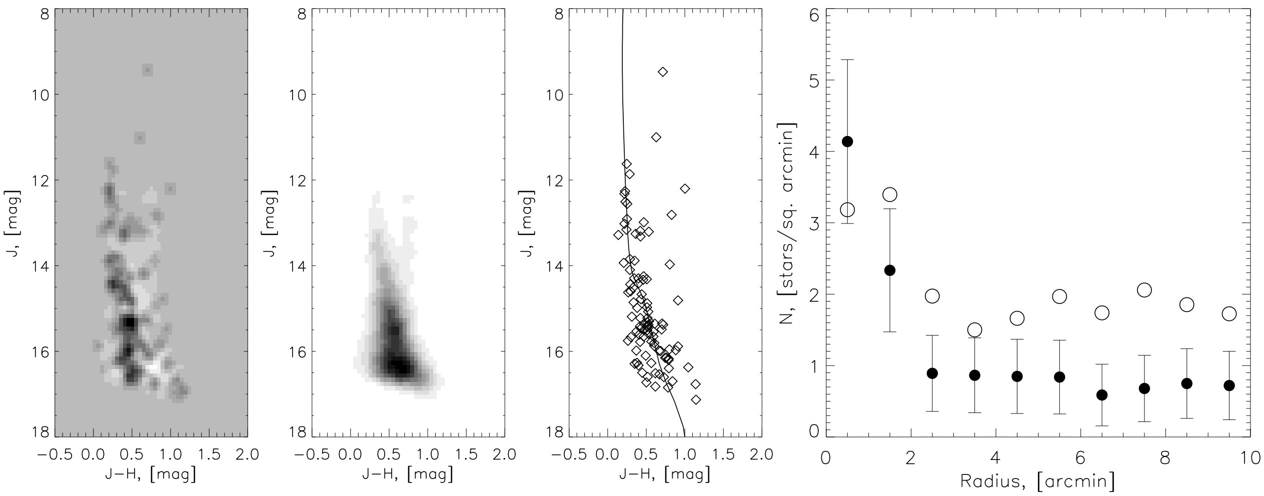

Fig. 6. Koposov 10 open cluster. First and second columns: Hess diagram of the Koposov 10 cluster and Hess diagram of the background. Third column: CMD diagram of the stars within 2′ from the center of the Koposov 10 with the fitted isochrone. Fourth column: Radial density distribution for Koposov 10, the symbols used are the same as on figure 5.

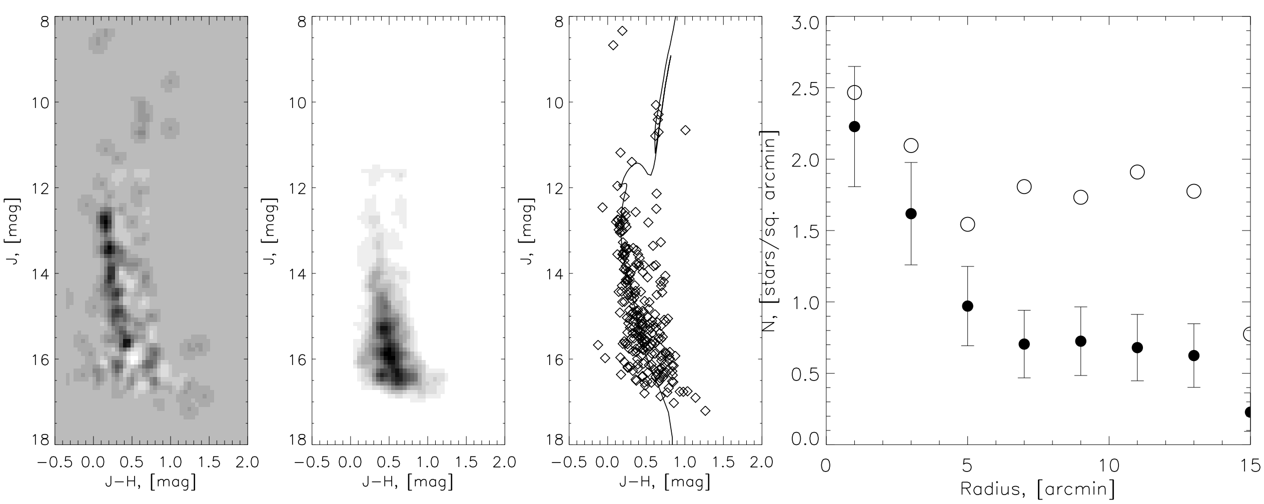

Fig. 7. Koposov 12 open cluster. First and second columns: Hess diagram of the Koposov 12 cluster and Hess diagram of the background. Third column: CMD diagram of the stars within 4′ from the center of the Koposov 12 with the fitted isochrone. Fourth column: Radial density distribution for Koposov 12, the symbols used are the same as on figure 5.

Table 2. Coordinates of new infrared embedded clusters

Name	RA (J2000) h:m:s	Dec (J2000) d:m:s	D arcsec
Koposov 7	05:40:44.1	+35:55:25	6
Koposov 41	06:03:58.0	+30:15:41	4
Koposov 58	05:51:11.0	+25:46:41	2
Koposov 82	06:11:55.8	+20:40:14	4

ters except Koposov 41. The Hess-diagram for this cluster exhibits the main sequence, and we can fit it with the isochrone of the age of 4 Myr. This best-fit isochrone was used to find the distance to amount to 2200 pc and the color excess $E(B-V) = 1.95$.

32 overdensities turned to be known clusters: 23 ones were matched to the objects from Dias catalog (Dias et al., 2002), and 9 ones, to IR clusters from the list by Bica et al. (2003a) and Bica et al. (2003b). 12 clusters have unreliable or no parameter measurements in the Dias catalog. We found the distances, ages, and reddenings for these objects (see Table 3). In some cases, we obtained more precise coordinates of the center of clusters, so we give new coordinates for all clusters. In the cases when Dias published reliable data, the physical parameters we determined using our technique are in a good agreement with the published ones.

In Table 4, we present the data on all clusters from the catalog by Dias et al. (2002), which have been detected by our technique on the square studied. Although two clusters, NGC 1912 and NGC 2168, have not been detected because of their large diameters (about 25 arcmin), we added their parameters to the table, as they exhibit slight overdensities and can be studied by our methods.

In the columns, we give parameters of the clusters both listed in the Dias catalog (Dias et al., 2002) and measured by applying our methodology to 2MASS catalog. For clusters Be 71, Be 72,

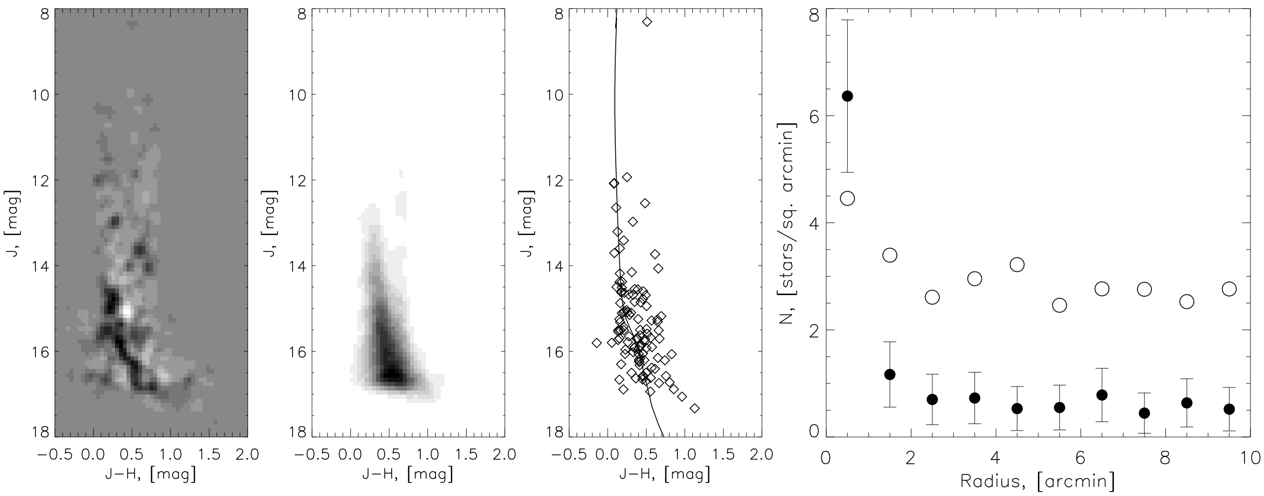

Fig. 8. Koposov 27 open cluster. First and second columns: Hess diagram of the Koposov 27 cluster and Hess diagram of the background. Third column: CMD diagram of the stars within 2′ from the center of the Koposov 27 with the fitted isochrone. Fourth column: Radial density distribution for Koposov 27, the symbols used are the same as on figure 5.

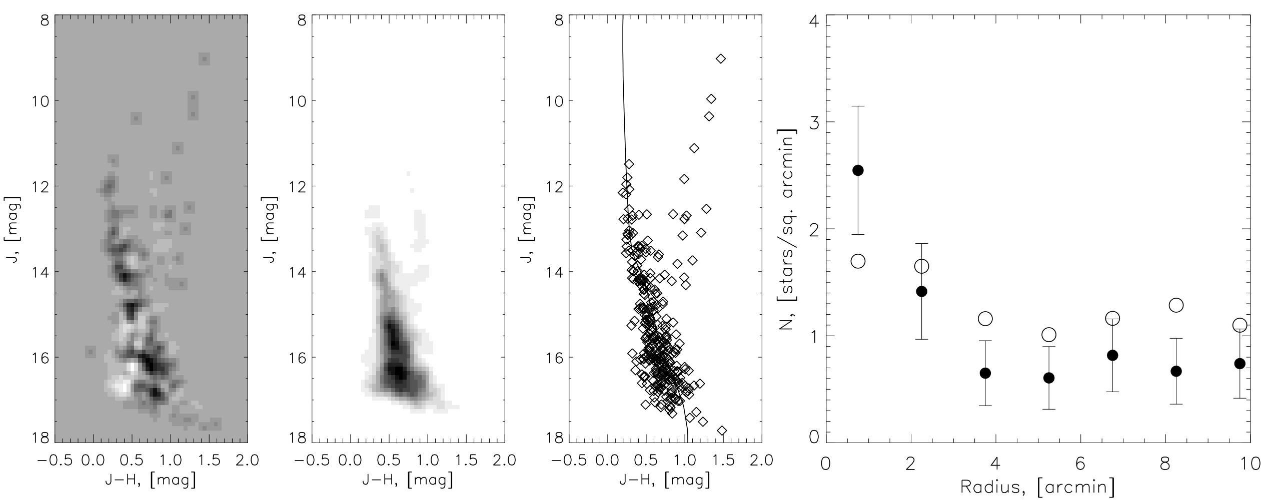

Fig. 9. Koposov 36 open cluster. First and second columns: Hess diagram of the Koposov 36 cluster and Hess diagram of the background. Third column: CMD diagram of the stars within 4′ from the center of the Koposov 36 with the fitted isochrone. Fourth column: Radial density distribution for Koposov 36, the symbols used are the same as on figure 5.

Cz 21, Cz 23, Cz 24, DC 8, Pis 27, Dias does not publish any parameters except their coordinates and diameters. However, in the WEBDA database there are data on Be 71 taken from the paper by Lata et al. (2004): $E(B-V) = 0.85$, $d = 3900pc$, $log(t) = 8.80$. It is seen that the color excess and the age well agree with our parameters, whereas the distance exceeds our value by 1500 pc. The difference in distance evaluations (when the age estimations are pretty close) can be attributed to the fact that the authors fitted $(V, B-V)$ CMD by ZAMS given by Schmidt-Kaler (1982) to estimate the distance modulus, and the theoretical isochrones given by Girardi et al. (2002) to find the cluster's age. Unlikely we used 2MASS theoretical isochrones by Girardi et al. (2002) to evaluate all cluster's parameters.

Parameters we measured for 7 clusters (Be 19, Kronberger 1, King 8, NGC 1931, Stock 8, NGC 1912 and NGC 2158), significantly differ from the data in the catalog by Dias et al. (2002), but we suppose our results are more precise and homogeneous. Parameters of Be 19 were obtained by Christian (1980) as following: employing the UBV photographic photometry data, the author compared the CMD of Be 19 with both the color-magnitude diagram of NGC 752 and the theoretical isochrones by Ciardullo (1979). Parameters of King 8 cluster appeared in the catalog by Dias et al. (2002) have been calculated by Loktin et al. (2001) using photographic photometry by Christian (1981). However, Christian (1981) published the distance to the clusters equal to 3.5 kpc, which essentially differs from the value of 6403 pc by Loktin et al. (2001). Parameters of Stock 8 were also obtained by Loktin et al. (2001) using the UBV photometry of 32 stars only measured by different authors; these stars do not show any sequence on CMD. As for clusters Kronberger 1, its isochrone corresponding to the parameters available in the catalog by Dias et al. (2002) fitted the main sequence of field stars, whereas the cluster members are noticeably shifted to the right on the CMD $(J, J-H)$ because of the extinc-

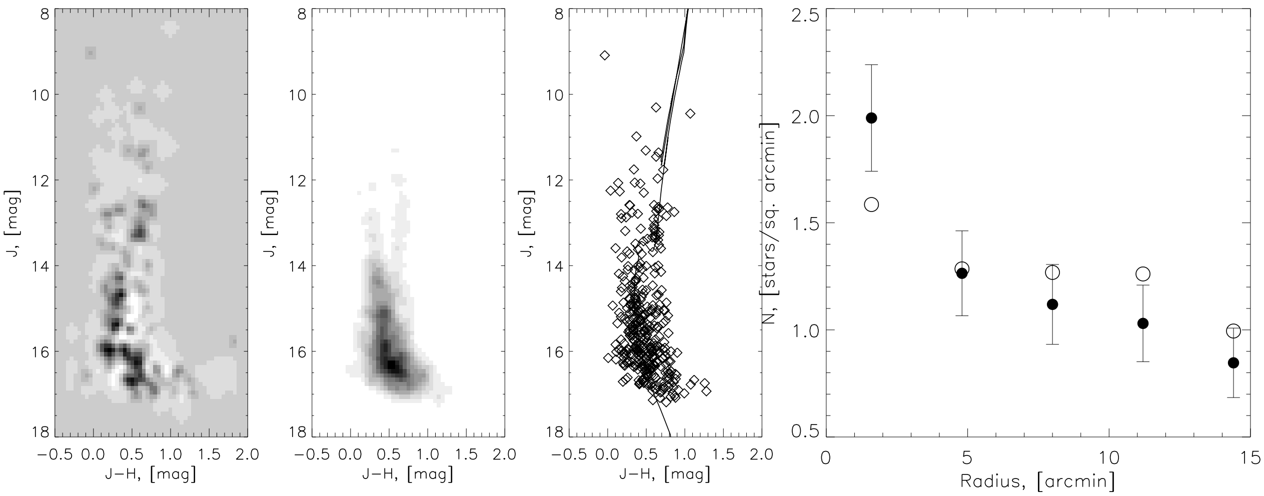

Fig. 10. Koposov 43 open cluster. First and second columns: Hess diagram of the Koposov 43 cluster and Hess diagram of the background. Third column: CMD diagram of the stars within 4′ from the center of the Koposov 43 with the fitted isochrone. Fourth column: Radial density distribution for Koposov 43, the symbols used are the same as on figure 5.

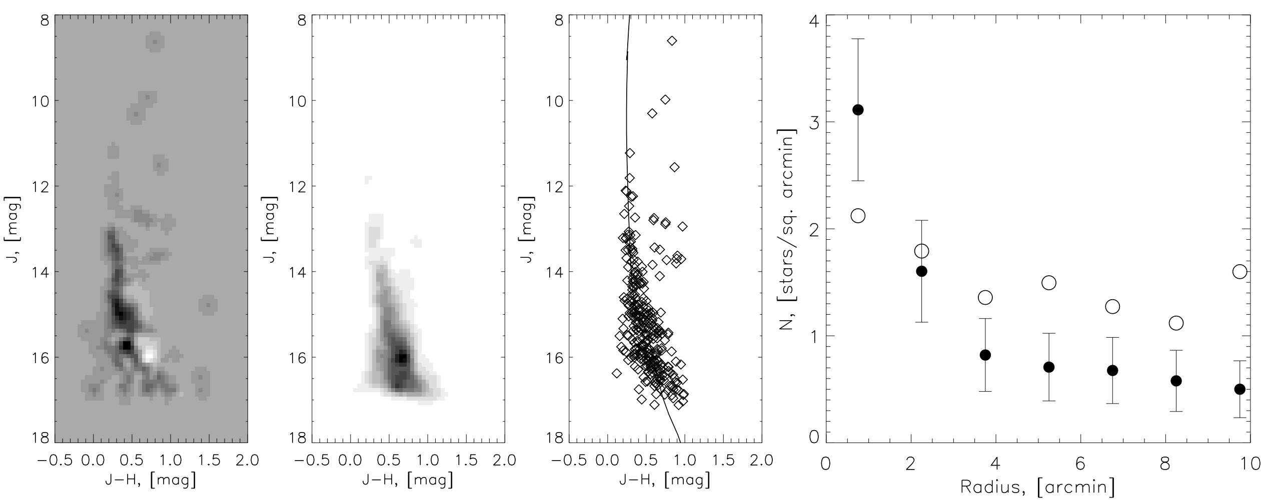

Fig. 11. Koposov 49 open cluster. First and second columns: Hess diagram of the Koposov 49 cluster and Hess diagram of the background. Third column: CMD diagram of the stars within 4′ from the center of the Koposov 49 with the fitted isochrone. Fourth column: Radial density distribution for Koposov 49, the symbols used are the same as on figure 5.

tion. The effect of extinction is clearly seen on the corresponding Hess-diagrams. The distance to the cluster NGC 1912 is in a good agreement with the distance by Dias et al. (2002), but the ages are different. According to the Hess-diagram and our fitting, the cluster is young. The population referred to as blue plume by Carraro et al. (2005) manifests itself on the Hess-diagram. Parameters of NGC 1931 cluster were obtained by Loktin et al. (2001) using published photometry data by Bhatt et al. (1994), but the authors themselves give the distance of 2170 pc. This cluster is embedded in a nebula, so its Hess-diagram shows a slightly scattered area occupied by the cluster. We fitted its CMD with a very young isochrone, and the distance appeared to be three times smaller than that by Dias et al. (2002). The estimations of the distance to NGC 2158 cluster differ from each other very noticeably (by 2 kpc). Dias et al. (2002) take data from the paper by Loktin et al. (2001), who used compilative data and automatic method to find the cluster's parameters. At the same time, our data are in good accordance with parameters by Carraro et al. (2002) who obtained 3600 pc for the distance, $E(B-V) = 0.55$, and $log(t) = 9.3$ by fitting isochrone from Girardi et al. (2000) and then comparing the best-fit with the simulated synthetic CMD. The discussion above demonstrates that the authors often publish controversial estimations of the cluster parameters even if they employ the same observational data. Although our estimations are sometimes based upon less deep photometric data, they have an essential advantage in homogeneity of both observational data and used isochrones and fitting methods.

Members of NGC 1893 cluster detected on the Hess-diagram do not lie on the same isochrone, so we cannot find a satisfactory fitting. This fact can be reasonably attributed to the existence of pre-main sequence stars in this cluster described by Vallenari et al. (1999). The distance to the cluster found by

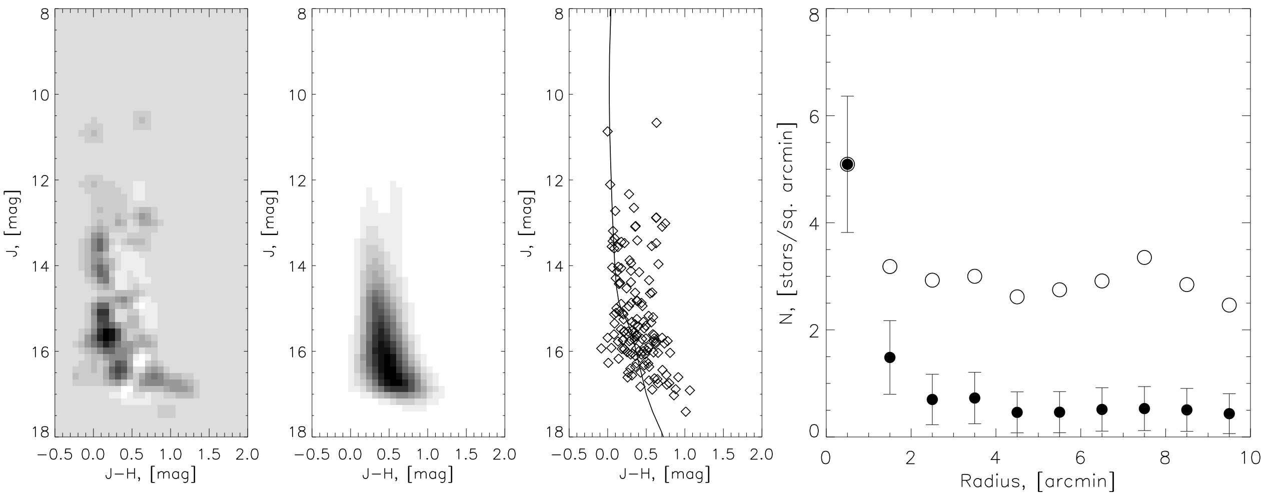

Fig. 12. Koposov 53 open cluster. First and second columns: Hess diagram of the Koposov 53 cluster and Hess diagram of the background. Third column: CMD diagram of the stars within 4′ from the center of the Koposov 53 with the fitted isochrone. Fourth column: Radial density distribution for Koposov 53, the symbols used are the same as on figure 5.

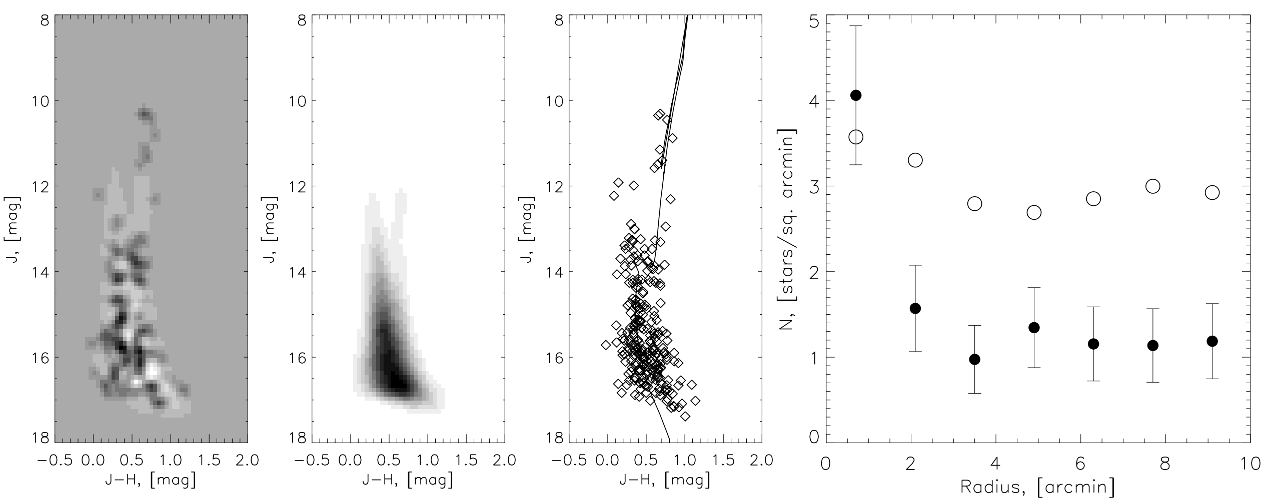

Fig. 13. Koposov 62 open cluster. First and second columns: Hess diagram of the Koposov 62 cluster and Hess diagram of the background. Third column: CMD diagram of the stars within 3′ from the center of the Koposov 62 with the fitted isochrone. Fourth column: Radial density distribution for Koposov 62, the symbols used are the same as on figure 5.

Vallenari et al. (1999) equals to 4300 pc (cf. with 6000 pc in the Dias catalog).

In the remaining 10 cases, our parameters closely agree (to within the error levels) with the corresponding data available from the catalog by Dias et al. (2002). These error levels are as follow: 200-500 pc for the distances, 0.10^m for the color excess $E(B-V)$, and 0.05 for $log(t)$. Here, we would like to specially note IC 2157 cluster: the Hess-diagram indicates that its main sequence abruptly terminates in the field of faint stars at $J = 15$.

Thus, out of 25 known clusters in the selected area, only in 10 cases we can accept the values of the cluster parameters listed in the catalog by Dias et al. (2002). There are five additional clusters which have parameters in Dias' catalog and which have not been detected in the field under study (see section 3). However, the distances and other parameters for four of them were obtained from very poor (V,B-V) diagrams which do not show any sequence or clump at the CMD, and we did not consider these clusters. Therefore, to get a catalog of homogeneously measured parameters of open clusters, it is necessary not only to search for new clusters and thoroughly investigate them, but also to recalculate the parameters of all known clusters using uniform raw datasets and a uniform and automated processing methodology.

At the end, 41 of 88 density peaks showed no evidence of being real clusters. In these cases, we detect either a nebula, or a bright star, or occasional groups of stars, whose density for some reasons exceeds the density of field stars.

Fig. 20 shows the distribution of all clusters under investigation across the galactic plane: both the newly opened clusters and the known ones, whose parameters were (re)determined in the present study. The crosses indicate the clusters with $log(age)$ less then 8.00; all young clusters are situated from 1 to 3.5 kpc from the Sun. As one can see from Fig. 20, the number of clusters in the square studied, for which their main physical param-

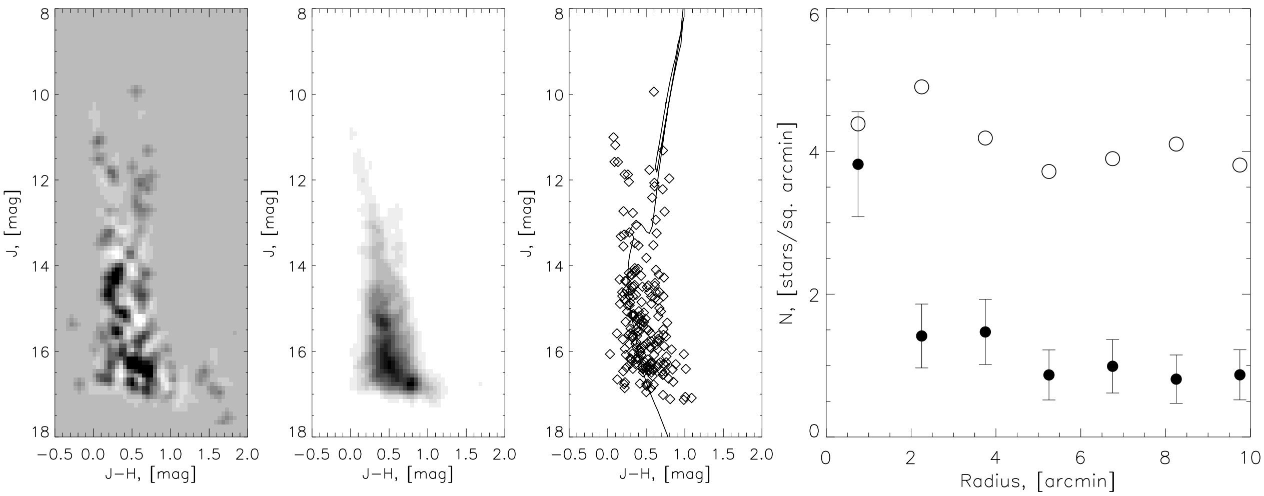

Fig. 14. Koposov 63 open cluster. First and second columns: Hess diagram of the Koposov 63 cluster and Hess diagram of the background. Third column: CMD diagram of the stars within $2'.5$ from the center of the Koposov 63 with the fitted isochrone. Fourth column: Radial density distribution for Koposov 63, the symbols used are the same as on figure 5.

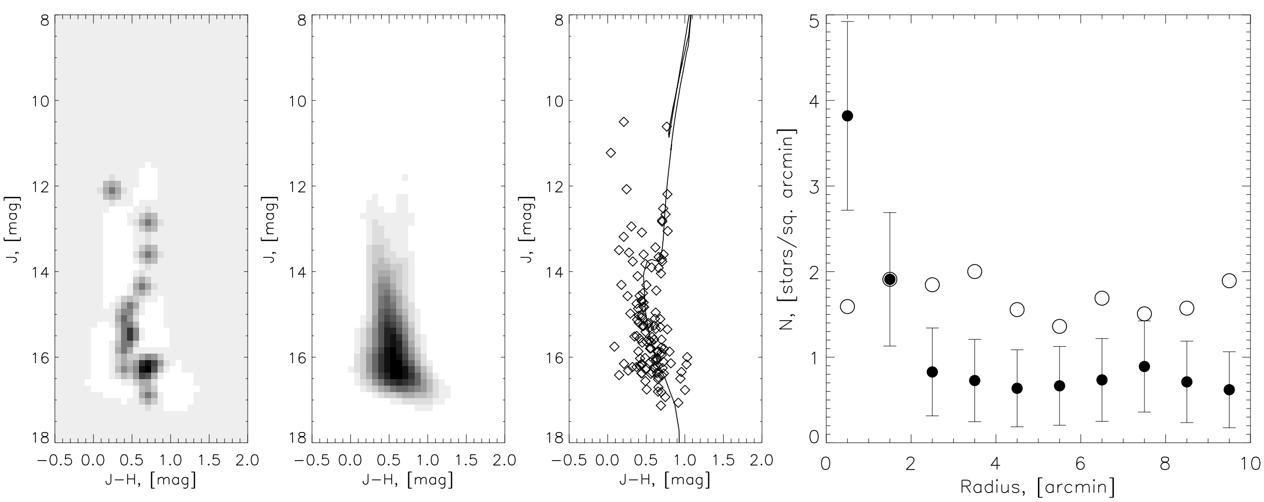

Fig. 15. Koposov 77 open cluster. First and second columns: Hess diagram of the Koposov 77 cluster and Hess diagram of the background. Third column: CMD diagram of the stars within $2'.5$ from the center of the Koposov 77 with the fitted isochrone. Fourth column: Radial density distribution for Koposov 77, the symbols used are the same as on figure 5.

eters are reliably evaluated, has increased from 11 in the catalog by Dias et al. (2002) (10 detected clusters plus one undetected) to 35 in our study.

5. Conclusions

We have demonstrated the new method of searching for star clusters in the data from large surveys and applied it to the 2MASS data. In the small field of 16 by 16 degrees in the poor region of Galactic anticenter, we have found and verified 15 new open clusters. For 12 of them, we obtained main physical parameters. For 14 previously known clusters, we have found or improved the distance, age and color excess. Currently, this method is being applied for all 2MASS data to create a uniform catalog of open clusters in our Galaxy.

Acknowledgements. The work was supported by the Russian Foundation for Basic Research (grant no. 05-02-16526) and the President Grant NSH-5290.2006.2. S. Koposov is supported by the DFG through SFB 439 and by a EARA-EST Marie Curie Visiting fellowship.

This research has made use of the SAI Catalog Access Services, Sternberg Astronomical Institute, Moscow, Russia.

This publication makes use of data products from the Two Micron All Sky Survey, which is a joint project of the University of Massachusetts and the Infrared Processing and Analysis Center/California Institute of Technology, funded by the National Aeronautics and Space Administration and the National Science Foundation.

We thank for Hans-Walter Rix, Vasily Belokurov and Wilton Dias for the comments on earlier versions of this paper.

References

Babaud J., A. P. Witkin, M. Baudin, and R. O. Duda. 1986, IEEE Trans. Pattern Anal. Mach. Intell., 8, 1, 26

Bica, E., Dutra, C. M., Soares, J., & Barbuy, B. 2003a, A&A, 404, 223

Bica, E., Dutra, C. M., & Barbuy, B. 2003b, A&A, 397, 177

Bhatt, B. C., Pandey, A. K., Mahra, H. S., & Paliwal, D. C. 1994, Bulletin of the Astronomical Society of India, 22, 291

Table 1. Parameters of new clusters

Name	RA (J2000) h:m:s	Dec (J2000) d:m:s	D arcsec	E(B-V) mag	$\frac{E(J-H)}{E(J-K)}$	$(m-M)_0$ mag	Distance pc	Age log(yr)
Koposov 10	05:47:28.6	+35:25:56	4	0.89±0.15	0.66	11.49±0.09	2000±80	<7.50
Koposov 12	06:00:56.2	+35:16:36	9	0.30±0.03	0.51	11.55±0.03	2050±50	8.90±0.05
Koposov 27	05:39:30.0	+33:21:00	3	0.60±0.03	0.57	12.77±0.11	3600±120	<7.50
Koposov 36	05:36:50.6	+31:12:39	9	0.91±0.16	0.67	10.91±0.09	1500±100	<7.50
Koposov 43	05:52:14.6	+29:55:09	8	0.38±0.10	0.44	12.21±0.09	2800±120	9.30±0.05
Koposov 49	05:44:22.2	+28:49:13	6	1.01±0.14	0.64	12.06±0.31	2600±400	<7.50
Koposov 52	05:53:48.9	+26:50:26	5	1.03±0.04	0.58	12.32±0.11	2900±140	8.95±0.05
Koposov 53	06:08:56.2	+26:15:49	5	0.38±0.01	0.55	12.68±0.38	3450±550	<7.55
Koposov 62	06:18:02.0	+24:42:38	6	0.34±0.02	0.57	12.21±0.05	2800±60	9.40±0.05
Koposov 63	06:10:01.7	+24:33:38	5	0.26±0.04	0.40	12.32±0.28	3000±350	9.15±0.05
Koposov 77	05:43:52.3	+21:42:37	5	0.57±0.01	0.55	11.23±0.02	1750±50	9.65±0.05

Table 3. Measured parameters of the clusters without counterparts in the Dias catalog

Name	RA (J2000) h:m:s	Dec (J2000) d:m:s	E(B-V) mag	$\frac{E(J-H)}{E(J-K)}$	$(m-M)_0$ mag	Distance pc	Age log(yr)
Berkeley 19	05:24:02.8	+29:34:16	0.61±0.05	0.72	12.38±0.40	3000±600	9.25±0.05
Berkeley 71	05:40:56.7	+32:16:33	0.91±0.05	0.58	11.94±0.18	2450±110	8.80±0.05
Berkeley 72	05:50:17.6	+22:14:59	0.43±0.01	0.57	12.72±0.20	3500±300	8.65±0.05
Czernik 21	05:26:41.0	+36:00:49	0.72±0.02	0.56	11.82±0.20	2300±200	9.55±0.05
Czernik 23	05:50:03.6	+28:53:41	0.38±0.02	0.53	12.00±0.04	2500±70	8.45±0.05
Czernik 24	05:55:24.6	+20:53:11	0.26±0.12	0.39	13.32±0.01	4600±10	9.40±0.05
DC 8	06:09:21.3	+31:13:54	0.72±0.06	0.73	11.62±0.40	2100±300	9.00±0.05
King 8	05:49:19.0	+33:37:38	0.44±0.04	0.50	12.47±0.13	3100±200	9.05±0.05
Kronberger 1	05:28:22.0	+34:46:24	0.43±0.10	0.72	9.60±0.30	800±100	<7.5
NGC 1931	05:31:25.9	+34:12:50	1.97±0.20	0.84	10.06±0.20	1000±120	<7.0
Pismis 27	06:10:53.8	+20:36:26	0.68±0.06	0.60	10.04±0.02	1000±10	<7.5
Stock 8	05:28:08.8	+34:25:53	1.21±0.04	0.57	9.84±0.20	900±110	<7.5

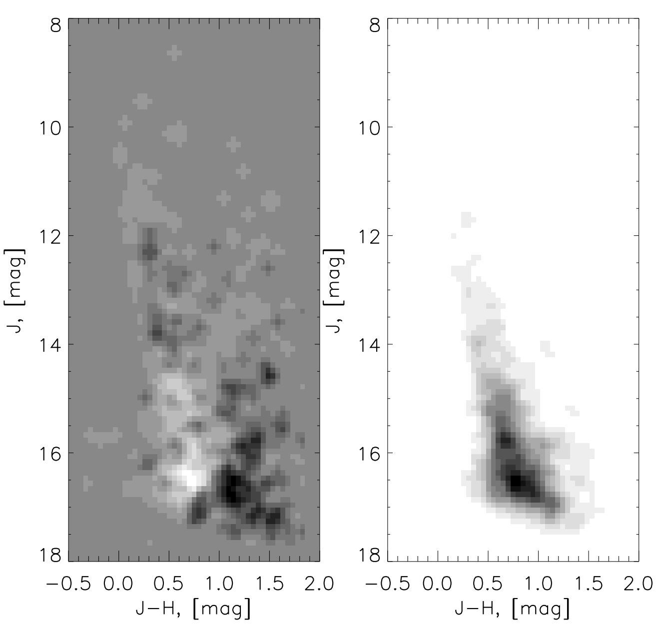

Fig. 16. Hess diagram of the IR embedded cluster Koposov 7 and Hess diagram of the background.

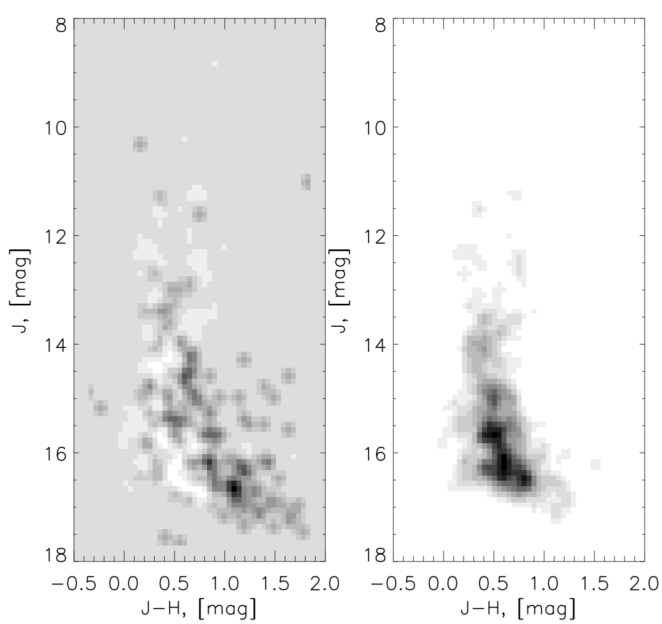

Fig. 17. Hess diagram of the IR embedded cluster Koposov 41 and Hess diagram of the background

Borissova, J., Pessev, P., Ivanov, V. D., Saviane, I., Kurtev, R., & Ivanov, G. R. 2003, A&A, 411, 83
Cardelli, J. A., Clayton, G. C., & Mathis, J. S. 1989, ApJ, 345, 245
Carraro, G., Girardi, L., & Marigo, P. 2002, MNRAS, 332, 705
Carraro, G., Vázquez, R. A., Moitinho, A., & Baume, G. 2005, ApJ, 630, L153
Ciardullo, R. B., & Demarque, P. 1979, In "Problems of Calibration of Multicolor Photometric Systems," Dudley Observatory 14, 317
Christian, C. A. 1980, AJ, 85, 700
Christian, C. A. 1981, ApJ, 246, 827
Dias, W. S., Alessi, B. S., Moitinho, A., & Lépine, J. R. D. 2002, A&A, 389, 871

Table 4. Comparison of physical parameters of the clusters: Dias catalog vs. present study

Name	Name$_{KG}$	RA(J2000) h:m:s	Dec(J2000) d:m:s	D_D pc	D_{KG} pc	$E(B-V)_D$ mag	$E(B-V)_{KG}$ mag	Age_D log(yr)	Age_{KG} log(yr)
Basel 4	Koposov 42	05:48:54.9	+30:11:08	3000	2750	0.45	0.57	8.30	8.25
Berkeley 17	Koposov 38	05:20:29.6	+30:34:33	2700	2400	0.58	0.30	10.00	10.00
Berkeley 19	Koposov 44	05:24:02.8	+29:34:16	4831	3000	0.40	0.61	9.49	9.25
Berkeley 21	Koposov 76	05:51:47.4	+21:48:31	5000	5150	0.76	0.51	9.34	9.35
Berkeley 69	Koposov 29	05:42:22.6	+22:50:01	2860	2900	0.65	0.45	8.95	9.00
Berkeley 71	Koposov 31	05:40:56.7	+32:16:33		2450		0.91		8.80
Berkeley 72	Koposov 74	05:50:17.6	+22:14:59		3500		0.43		8.65
Czernik 21	Koposov 6	05:26:41.0	+36:00:49		2300		0.72		9.55
Czernik 23	Koposov 48	05:50:03.6	+28:53:41		2500		0.38		8.45
Czernik 24	Koposov 80	05:55:24.6	+20:53:11		4600		0.26		9.40
DC 8	Koposov 35	06:09:21.3	+31:13:54		2100		0.72		9.00
IC 2157	Koposov 65	06:04:41.9	+24:06:01	2040	2400	0.548	0.58	7.800	<7.0
King 8	Koposov 24	05:49:19.0	+33:37:38	6403	3100	0.580	0.44	8.618	9.05
Kronberger 1	Koposov 15	05:28:22.0	+34:46:24	1900	800	0.52	0.43	7.5	<7.5
NGC 1893	Koposov 25	05:22:53.7	+33:26:17	6000		0.45		6.48	
NGC 1907	Koposov 11	05:28:10.7	+35:19:44	1800	1300	0.52	0.51	8.5	8.60
NGC 1931	Koposov 20	05:31:25.9	+34:12:50	3086	1000	0.738	1.97	7.002	<7.0
NGC 1960	Koposov 21	05:36:19.6	+34:07:27	1330	1050	0.22	0.19	7.4	<7.5
NGC 2099	Koposov 30	05:52:18.4	+32:33:03	1383	1300	0.302	0.27	8.540	8.60
NGC 2129	Koposov 68	06:01:10.5	+23:19:34	2200	1950	0.80	0.82	7.00	<7.5
NGC 2158	Koposov 64	06:07:27.8	+24:05:53	5071	3300	0.360	0.34	9.023	9.30
Pismis 27	Koposov 86	06:10:53.8	+20:36:26		1000		0.68		<7.5
Stock 8	Koposov 18	05:28:08.8	+34:25:53	1821	900	0.445	1.21	7.056	<7.5
NGC 1912		05:28:41.6	+35:48:34	1400	1000	0.25	0.38	8.5	<7.3
NGC 2168		06:09:00.0	+24:21:00	912	900	0.20	0.19	8.25	<7.5

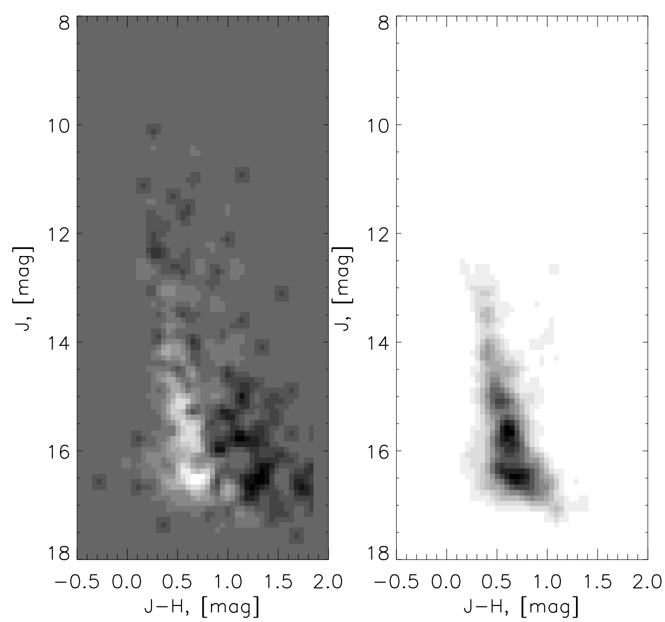

Fig. 18. Hess diagram of the IR embedded cluster Koposov 58 and Hess diagram of the background

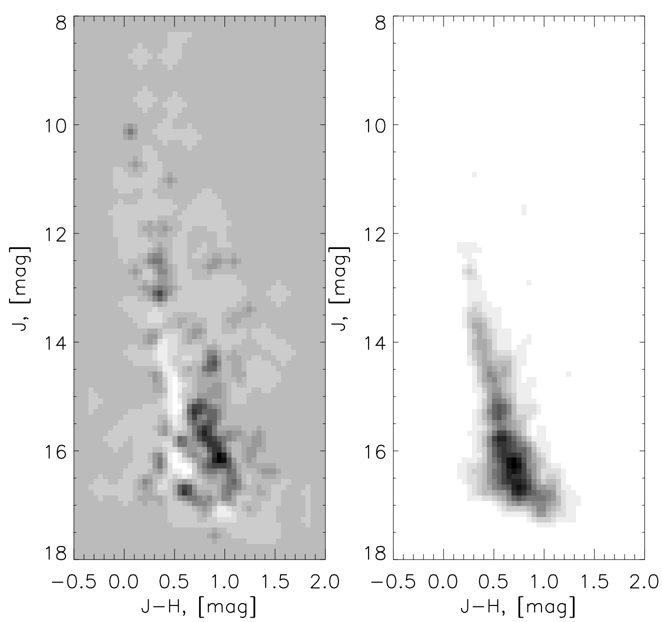

Fig. 19. Hess diagram of the IR embedded cluster Koposov 82 and Hess diagram of the background

Drake, A. J. 2005, A&A, 435, 545
Dutra, C. M., Santiago, B. X., & Bica, E. 2002, A&A, 381, 219
Dutra, C. M., Bica, E., Soares, J., & Barbuy, B. 2003, A&A, 400, 533
Froebrich, D., Scholz, A., Raftery, C. L. 2006, astro-ph/0610146
Girardi, L., Bressan, A., Bertelli, G., & Chiosi, C. 2000, A&AS, 141, 371
Girardi, L., Bertelli, G., Bressan, A., Chiosi, C., Groenewegen, M. A. T., Marigo, P., Salasnich, B., & Weiss, A. 2002, A&A, 391, 195
Ivanov, V. D., Borissova, J., Pessev, P., Ivanov, G. R., & Kurtev, R. 2002, A&A, 394, L1
Koposov, S. E., & Bartunov, O. S. 2006, The Virtual Observatory in Action: New Science, New Technology, and Next Generation Facilities, 26th meeting of the IAU, Special Session 3, 17-18, 21-22 August, 2006 in Prague, Czech Republic, SPS3, #19, 3,
Koposov, S., Glushkova, E., & Zolotukhin, I. 2005, Astronomische Nachrichten, 326, 597
Koposov, S., et al. 2007, ArXiv e-prints, 706, arXiv:0706.0019, accepted to ApJ
Koposov, S., et al. 2007, ArXiv e-prints, 706, arXiv:0706.2687, submitted to ApJ
Kronberger, M., et al. 2006, A&A, 447, 921

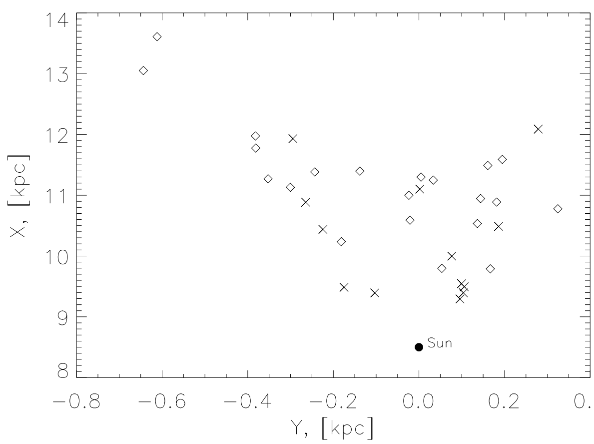

Fig. 20. Distribution of clusters across the galactic plane. The crosses denote the clusters younger than 100 Myr, while the diamonds denote the clusters older than 100 Myr.

Lata, S., Mohan, V., & Sagar, R. 2004, Bulletin of the Astronomical Society of India, 32, 371
Lindenberg, T., 1998, International Journal of Computer Vision, 30, 2, 79
Loktin, A. V., Gerasimenko, T. P., & Malisheva L. K. 2001, Astron. Astrophys. Trans. 20, 607
Schmidt-Kaler Th. 1982, in Scaifers K., Voigt H. H., eds, Landolt/Bornstein, Numerical Data and Functional Relationship in Science and Technology, New series, Group VI, Vol. 2b. Springer-Verlag, Berlin, Pp. 14.
Skrutskie, M. F., et al. 2006, AJ, 131, 1163
Surdin, V. G. 2000, Formación estelar, Editorial URSS, Moscú, 272p.
Vallenari, A., Richichi, A., Carraro, G., & Girardi, L. 1999, A&A, 349, 825
Zolotukhin, I., Koposov, S., & Glushkova, E. 2006, ASP Conf. Ser. 351: Astronomical Data Analysis Software and Systems XV, 351, 240